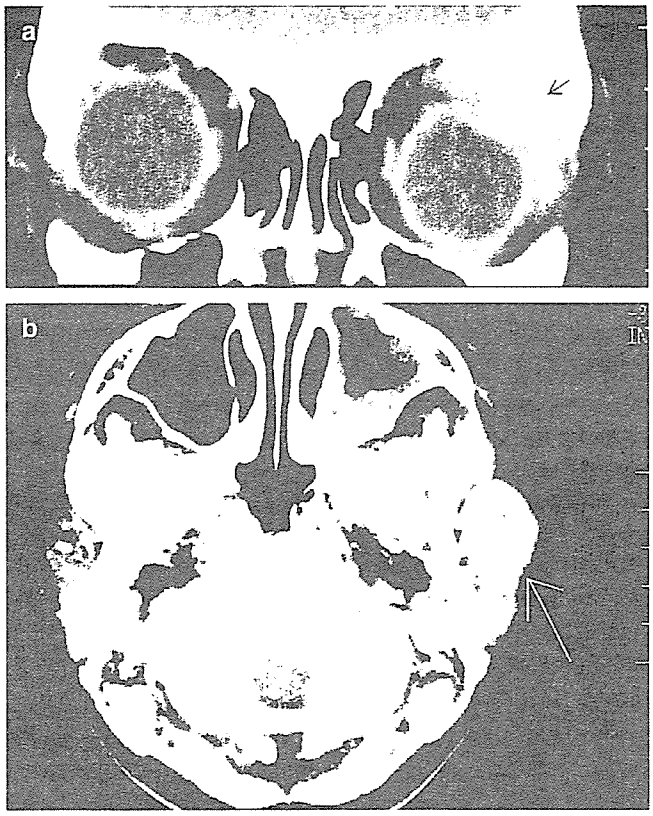

Figure 1 Radiological appearance. (**a**) The initial tumor mass (arrow) is visible in the left upper lateral aspect of the orbital region as a partially calcified, low-density mass on a CT image. (**b**) CT of the first recurrence showing an irregular mass (arrow) with a central low-density area near the upper aspect of the left parotid gland.

although the possibility of future recurrence cannot be ruled out.

PATHOLOGICAL FINDINGS

A conventional morphological examination was performed using formalin-fixed paraffin sections stained with HE. Histological examination of the primary tumor suggested an epithelial neoplasm, like a lacrimal gland carcinoma or an adenoid cystic carcinoma, or a rhabdomyosarcoma or metastasis of an abdominal tumor. The first recurrent tumor was characterized by conspicuously atypical small cell proliferation, forming solid cellular nodules or trabecular, basalioid epithelial lesions, and was accompanied by prominent interstitial fibrous intervention (Fig. 2). The tumorous tissue was intermingled with the ducts of the parotid gland, and the tumor itself was located adjacent to the serous acini of the parotid gland. The second recurrent main tumor exhibited diffuse cellular proliferation but did not have a desmoplastic stroma. The nodal metastases in the lower portion of the left neck, however, exhibited a distinct desmoplastic morphology similar to that of the first recurrent tumor. These histological findings were consistent with a desmoplastic small cell tumor of soft tissue with divergent differentiation, and were almost identical to those of the initial orbital tumor.

Immunohistochemical study

The immunohistochemical investigation was performed using formalin-fixed, paraffin-embedded tissues and the streptoavidin–biotin peroxidase indirect method. Primary antibodies were prepared against the following antigens: desmin (clone DE-R-11, diluted 1:50; DakoCytomation, Glostrup, Denmark), cytokeratin (AE1/AE3, diluted 1:50, proteinase K-treated; DakoCytomation), vimentin (Vim3B4, diluted 1:50, microwave-treated; DakoCytomation), epithelial membrane antigen (EMA; E29, diluted 1:50; DakoCytomation), myogenin (F5D, diluted 1:50, microwave-treated; DakoCytomation), WT1 (C-19, diluted 1:50, proteinase K-treated; Santa Cruz Biotechnology, Santa Cruz, CA, USA), CD99 (F5D, diluted 1:50; DakoCytomation), sarcomeric actin (α-Sr-1, diluted 1:40; DakoCytomation), CD45 (T29/33, diluted 1:50; DakoCytomation), glial fibrillary acidic protein (GFAP; 6F2, diluted 1:50, microwave-treated; DakoCytomation), neuron-specific enolase (NSE; BBS/NC/VI-H14, diluted 1:50; DakoCytomation), S-100 protein (rabbit polyclonal, diluted 1:400; DakoCytomation), Ki-67 antigen (MIB-1, diluted 1:50, microwave-treated; DakoCytomation), and P53 (PAb240, diluted 1:50, microwave-treated; DakoCytomation).

The solid areas of the first and second recurrent tumors were positive for vimentin, but the trabeculae were negative. In contrast, the trabecular or epithelioid components were positive for EMA, but the solid cellular area was negative. Distinct positive immunoreactivity for desmin and cytokeratin was expressed in the cytoplasm of the small tumor cells in both the solid cellular and trabecular architectures (Fig. 3). No evidence of myogenin, WT1, CD99, sarcomeric actin, CD45, GFAP, NSE, or S-100 protein positivity was seen. Ki-67 labeling index was 40–60% in the solid area of tumor and 10–20% at the trabeculae. P53 labeling index was <1–5%.

Electron microscopy

The electron microscopy specimens were prepared using conventional 2% glutaraldehyde and 1% osmium tetraoxide fixation followed by epoxy embedding. Ultrathin sections stained with uranyl acetate and lead citrate were then observed using a JEM 1010 transmission electron microscope (JEOL, Tokyo, Japan).

The tumor cells were characterized by prominent desmosome-type intercellular junctions with tonofilaments (Fig. 4). A small amount of intermediate fibrils without striated muscle

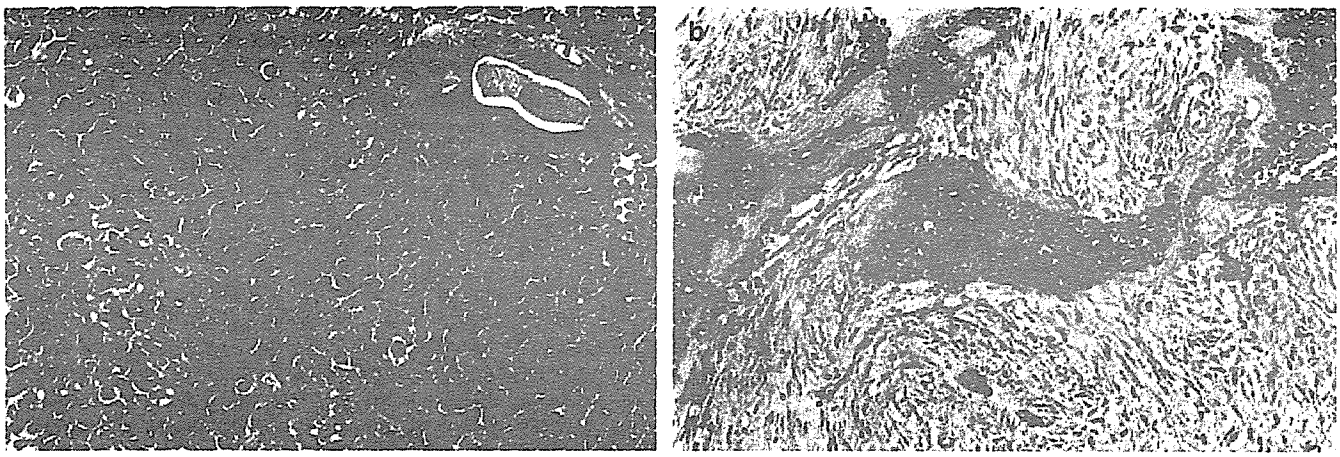

Figure 2 Histological findings. (**a**) Conspicuous proliferation of small atypical cells with increased mitotic figures is apparent. A salivary gland duct is visible at the right of the figure. (**b**) The tumor tissue is characterized by trabecular, epithelioid proliferation surrounded by a hyaline basal structure, with fibrous proliferation in the interstitium.

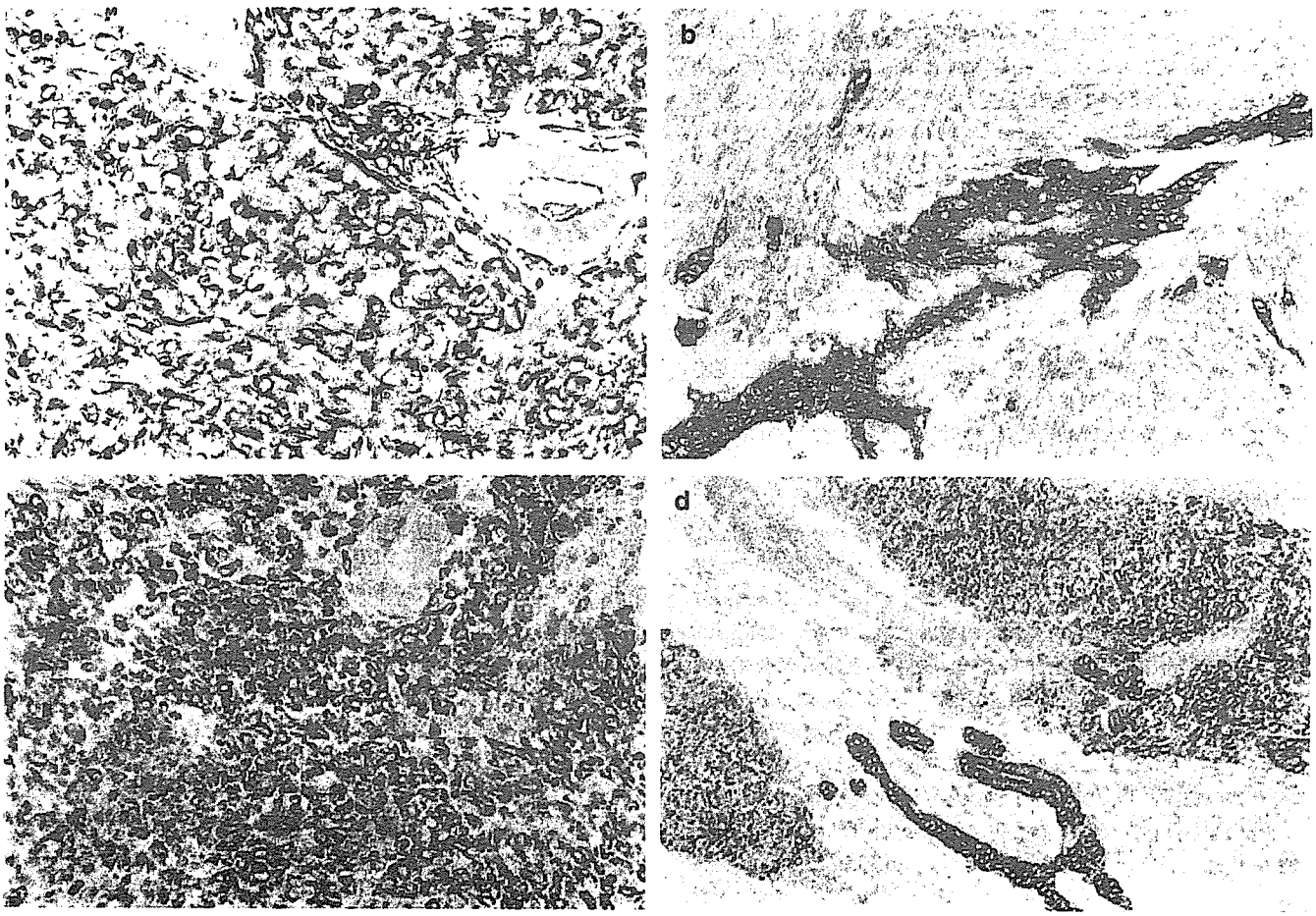

Figure 3 Immunohistochemical findings. (**a**) Vimentin is reactive in the cytoplasm of the tumor cells. (**b**) EMA is positive at the membrane of the tumor cells, especially in the trabecular region. Immunostaining was positive for (**c**) desmin and (**d**) cytokeratin in both solid and trabecular portions of the tumor.

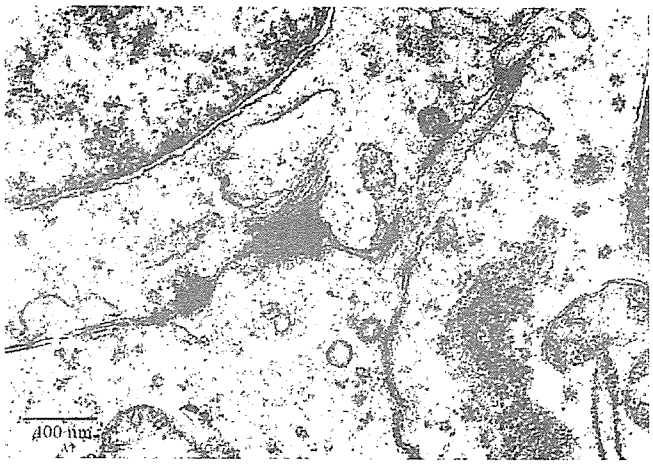

Figure 4 Electron microscopy. The tumor cells exhibit intercellular desmosomes with distinct tonofilaments.

differentiation were seen in the cytoplasm. No specific neurosecretory vesicle was found in the cytoplasm.

Gene analysis

Total RNA was extracted from frozen tumor tissue using an RNeasy Kit (Qiagen, Hilden, Germany) and was reverse transcribed to cDNA using a First-Strand cDNA synthesis Kit (Amersham, Piscataway, NJ, USA). PCR was performed using the following primers: EWS/WT1, ESBP1 (CGAC TAGTTATGATCAGAGCAGT)[2] and 10BA (TGCTGCCTGG GACACTGAAC); EWS-FLI1, 22.3 (TCCTACAGCCAAGCT CCAAGTC)[3] and 11.3 (ACTCCCCGTTGGTCCCCTCC); and EWS/ERG, ESBP1 and EU15 (CATGTACGGGAGGTCT GAGGGGT).[4] The amplified products were run on a 2% agarose gel. The products were then purified using MicroSpin S-400 Columns (Amersham) and cloned into pGEM-T vectors via the pGEM-T Vector System (Promega, Madison, WI, USA). Sequencing of the subcloned PCR products was performed using a DyEnamic ET Terminator Cycle Sequencing Kit (Amersham) with M13-40 and reverse primers.

The aforementioned histological diagnosis was also confirmed by RT-PCR of snap-frozen tumor tissues taken from the first recurrent tumor and the second recurrent masses, including both the solid cellular portion and the desmoplastic portion (Fig. 5). Each tissue specimen exhibited the same *EWS-WT1* chimeric fusion (data not shown). The chimeric transcript was finally confirmed by cloning and sequencing of the PCR product, resulting in the identification of an in-frame fusion of *EWS* exon 9 and *WT1* exon 8 (Fig. 6). Neither *EWS-FLI1* nor *EWS-ERG* chimeric transcripts associated with the Ewing family of tumors were detected (data not shown).

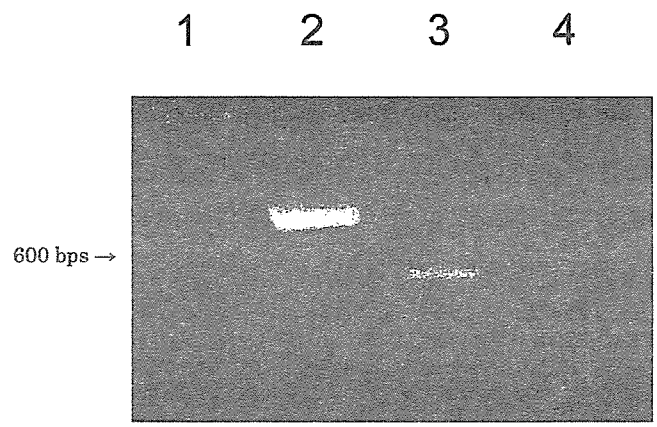

Figure 5 Molecular analysis. Reverse transcriptase–polymerase chain reaction of the first recurrent tumor tissue shows an in-frame fusion of *EWS* and *WT1* in lane 2, which contains a longer band than that of the positive desmoplastic small cell tumor (DSCT) control. A smaller product, corresponding to the fusion of *EWS* exon 7 to *WT1* exon 8, is also visible. Lane 1, 100 bp ladder marker; lane 2, present case; lane 3, positive DSCT control; lane 4, *NCR-NB3* negative control neuroblastoma cell.

	EWS exon 9	WT1 exon 8
Present case	cgaggtggcttcaataagcctggtg	gtgagaaaccataccagtgtgactt

Figure 6 Sequence of *EWS-WT1* junction. The fusion point of the longer product is shown. A vertical line indicates the nucleotide position of the junction.

DISCUSSION

Several epithelial neoplasms, many of which are malignant in adults, were initially considered in the differential diagnosis of the slow-growing tumor and repeated recurrences seen in the present case. Several kinds of malignant small cell tumors of soft tissues including rhabdomyosarcoma (especially alveolar type), extraskeletal Ewing sarcoma family of tumors (ESFT),[5] neuroblastoma metastases, and non-Hodgkin lymphoma (in addition to DSCT) must be ruled out in pediatric patients. The immunohistochemical reactivity of desmin or vimentin was not necessary to confirm a diagnosis of rhabdomyosarcoma because myogenin, which is a myogenic regulatory protein, was not reactive. The absence of CD99, CD45, NSE, S100, and GFAP reactivity enabled ESFT, non-Hodgkin lymphoma, and neuronal tumors to be ruled out. Electron microscopy revealed an epithelioid fine structure with distinct desmosomes, similar to the findings for a previously reported extra-abdominal DSCT.[6] No evidence of intracytoplasmic neurosecretory vesicles, often seen in neuroblastomas, or aggregates of thick myofilaments with electron-dense zones, indicating rhabdomyosarcoma, was found.

Another possibility in the differential diagnosis of small round cell tumors in children is DSCT. Recently, intra-

abdominal DSCT was recognized as a small cell tumor that usually occurs in the intra-abdominal region of children or young adults. DSCT is characterized by small cell proliferation, prominent stromal desmoplasia, and intra-abdominal serosal involvement. A distinct molecular property of this tumor is the presence of an in-frame fusion of the *EWS* gene and the *WT1* gene.[7–11]

Intra-abdominal DSCT has been described in the retroperitoneum, pancreatic region, gastric wall, and the pelvic, mesenteric, and omental regions.[7,9,12] Light microcopy has revealed a divergent differentiation pattern (small cell proliferation in an intermingled pattern) because the majority of cases exhibit a trabecular, basalioid, or glandular architecture associated with abundant interstitial fibrous proliferation, and, in some cases, solid cellular areas.[7] The small cells are typically positive for cytokeratin, EMA, vimentin, desmin, or NSE immunohistochemical staining.[7] Immunoreactivity for S100, Leu7, or LeuM1 has been observed in some cases.[6,13–20]

Cytogenetic investigation of intra-abdominal DSCT has revealed a consistent chromosomal translocation: t(11;22)(p13;q12). This translocation causes an in-frame fusion between the *EWS* gene and the *WT1* gene, producing a chimeric transcript. In most cases of intra-abdominal DSCT, the first seven exons of *EWS* are fused to the last three exons of *WT1*. *EWS-ERG* or *EWS-FLI1* fusion transcripts have also been described in some DSCT cases.[10–12,21]

The soft-tissue tumor in the present case was similarly characterized by divergent immunoreactivity pattern of EMA, cytokeratin, desmin, and vimentin in the solid and trabecular areas of the tumor. Electron microscopy showed the tumor cells to be arrayed with distinct desmosome-type intercellular junctions[6] and with intracytoplasmic intermediate fibrils in a few cells. These characteristics were morphologically and immunohistochemically consistent with a diagnosis of DSCT, despite the extra-abdominal location of the tumor. Molecular analysis of the first and second recurrent tumors showed the same in-frame fusion transcript, even though the tumor tissues had different morphological phenotypes.

Extra-abdominal DSCT is extremely rare, although ovarian or paratesticular involvement has been described.[13–15] DSCT of the soft tissue and bone of the hand, intracranial DSCT, and pleural cavity DSCT have also been reported.[16–19] To the best of our knowledge, no extra-abdominal DSCT confirmed by RT-PCR to exhibit an *EWS-WT1* chimeric fusion have been reported in Japanese studies. The morphological, immunohistochemical, ultrastructural, and molecular features of soft-tissue DSCT are similar to those of intra-abdominal DSCT. Gerald *et al.* reviewed and summarized 109 cases of DSCT, of which 103 were located in the abdominal cavity, four were in the thoracic region, one was in the cranial fossa, and one was in the hand.[20] Swanson *et al.* described 12 cases of polyphenotypic small cell tumors in children; two of these tumors arose from bone, six arose from soft tissue or the axial skeleton, two arose from the CNS, and two arose from the retroperitoneum.[1] All of the tumors exhibited primitive round cell features or neuroectodermal characteristics with or without myogenic, epithelial, or combined differentiation.

The present patient exhibited an uncommon form of the *EWS-WT1* fusion transcript: a fusion of *EWS* exon 9 and *WT1* exon 8, instead of the more common fusion of *EWS* exon 7 and *WT1* exon 8 seen in intra-abdominal DSCT.[8,22] Interestingly, two cases of DSCT of soft tissue and bone and one case of DSCT of the kidney exhibited the same type of fusion transcript.[6,19,23] This molecular aberration might be a variant of the in-frame *EWS-WT1* fusion transcript, because the *EWS-WT1* fusion gene has been reported to exhibit molecular heterogeneity, such as the fusion of *EWS* exon 10 and *WT1* exon 8[24] or the fusion of *EWS* exon 7 and *WT1* exon 9.[12] In contrast, intra-abdominal DSCT with a fusion of *EWS* exon 9 and *WT1* exon 8 has not been previously described. Furthermore, in spite of the cytological heterogeneity of the tumor phenotypes in the present case, the same in-frame *EWS-WT1* fusion was noted in the solid area and the desmoplastic epithelioid region. The genetic findings in the present case suggest that fusion gene heterogeneity may be related to the tissue-specific phenotypes of DSCT, although further investigation of other cases of extra-abdominal DSCT is needed to confirm this speculation.

ACKNOWLEDGMENTS

The authors wish to thank Dr Jun-ichi Mimaya, Dr Shuzo Park, and Dr Chin-Ying Lo (Departments of Oncology, Plastic Surgery, and Ophthalmology, Shizuoka Children's Hospital) and Dr Nobutada Katori and Dr Yasuhisa Nakamura (Department of Oculoplastic Surgery, Seirei Hamamatsu General Hospital) for kindly contributing this case and providing the follow-up information. The authors also thank Mr Naoshi Ishikawa and Mr Motohiro Sano (Department of Clinical Pathology and Laboratory Medicine, Shizuoka Children's Hospital) for their excellent technical assistance.

REFERENCES

1 Swanson PE, Dehner LP, Wick MR. Polyphenotypic small cell tumors of childhood [Abstract]. *Lab Invest* 1988; **58**: 9.
2 May W, Gishizky ML, Lessnick S *et al.* Ewing sarcoma 11;22 translocation produces a chimeric transcription factor that requires the DNA-binding domain encoded by FLI1 for transformation. *Proc Natl Acad Sci USA* 1993; **90**: 5752–6.
3 Delattre O, Zucman J, Plougastel B *et al.* Gene fusion with an ETS DNA-binding domain caused by chromosome translocation in human tumours. *Nature* 1992; **359**: 162–5.

4 Urano F, Umezawa A, Yabe H et al. J. Molecular analysis of Ewing's sarcoma: Another fusion gene, EWS-E1AF, available for diagnosis. *Jpn J Cancer Res* 1998; **89**: 703–11.
5 Delattre O, Zuckman J, Melot T *et al.* The Ewing family of tumors: A subgroup of small-round-cell tumors defined by specific chimeric transcripts. *N Engl J Med* 1994; **331**: 294–9.
6 Adsay V, Cheng J, Athanasian E *et al.* Primary desmoplastic small cell tumor of soft tissues and bone of the hand. *Am J Surg Pathol* 1999; **23**: 1408–13.
7 Gerald WL, Miller HK, Battifora H *et al.* Intra-abdominal desmoplastic small round-cell tumor. Report of 19 cases of a distinctive type of high-grade polyphenotypic malignancy affecting young individuals. *Am J Surg Pathol* 1991; **15**: 499–513.
8 Ladanyi M, Gerald W. Fusion of the EWS and WT1 genes in the desmoplastic small round cell tumor. *Cancer Res* 1994; **54**: 2837–40.
9 Murray JC, Minifee PK, Trautwein LM *et al.* Intraabdominal desmoplastic small round cell tumor presenting as a gastric mural mass with hepatic metastases. *J Pediatr Hematol Oncol* 1996; **18**: 289–92.
10 Ordi J, de Alava E, Torne A *et al.* Intraabdominal desmoplastic small round cell tumor with EWS/ERG fusion transcript. *Am J Surg Pathol* 1998; **22**: 1026–32.
11 Slominski A, Wortzman J, Carlson A *et al.* Molecular pathology of soft tissue and bone tumors. *Arch Pathol Lab Med* 1999; **123**: 1246–59.
12 Bismar TA, Basturk O, Gerald WL *et al.* Desmoplastic small cell tumor in the pancreas. *Am J Surg Pathol* 2004; **28**: 808–12.
13 Young RH, Eichhorn JH, Dickersin GR *et al.* Ovarian involvement by the intraabdominal desmoplastic small round cell tumor divergent differentiation: A report of three cases. *Hum Pathol* 1992; **23**: 454–64.
14 Resnick MB, Donovan M. Intra-abdominal desmoplastic small round cell tumor with extensive extra-abdominal involvement. *Pediatr Pathol Lab Med* 1995; **15**: 797–803.
15 Cumming OW, Ulbright TM, Young RH *et al.* Desmoplastic small round cell tumors of the paratesticular region. *Am J Surg Pathol* 1997; **21**: 219–25.
16 Parkash V, Gerald WL, Parma A *et al.* Desmoplastic small round cell tumor of the pleura. *Am J Surg Pathol* 1995; **19**: 659–65.
17 Tison V, Cerasoli S, Morigi F *et al.* Intracranial desmoplastic small-cell tumor. Report of a case. *Am J Surg Pathol* 1996; **20**: 112–17.
18 Venkateswaran L, Jenkins JJ, Kaste SC *et al.* Disseminated intrathoracic desmoplastic small round-cell tumor: A case report. *J Pediatr Hematol Oncol* 1997; **19**: 172–5.
19 Antonescu CR, Gerald WL, Magid MS *et al.* Molecular variants of the EWS-WT1 gene fusion in desmoplastric small round cell tumor. *Diagn Mol Pathol* 1998; **7**: 24–8.
20 Gerald WL, Ladanyi M, de Alava E *et al.* Clinical, pathologic, and molecular spectrum of tumors associated with t(11;22)(p13;q12): Desmoplastic small round-cell tumor and its variants. *J Clin Oncol* 1998; **16**: 3028–36.
21 Hill DA, O'Sullivan MJ, Zhu X *et al.* Practical application of molecular genetic testing as an aid to the surgical pathologic diagnosis of sarcomas. A prospective study. *Am J Surg Pathol* 2002; **26**: 965–77.
22 De Alava E, Landanyi M, Rosai J *et al.* Detection of chimeric transcripts in desmoplastic small round cell tumor and related developmental tumors by reverse transcriptase polymerase chain reaction. A specific assay. *Am J Pathol* 1995; **147**: 1584–91.
23 Su MC, Jeng YM, Chu YC. Desmoplastic small round cell tumor of the kidney. *Am J Surg Pathol* 2004; **28**: 1379–83.
24 Shimizu Y, Mitsui T, Kawakami T *et al.* Novel breakpoint of the EWS gene and the WT1 gene in a desmoplastic small round cell tumor. *Cancer Genet Cytogenet* 1998; **106**: 156–8.

Association of 11q Loss, Trisomy 12, and Possible 16q Loss with Loss of Imprinting of Insulin-Like Growth Factor–II in Wilms Tumor

Naoki Watanabe,[1,2] Hisaya Nakadate,[3] Masayuki Haruta,[1] Waka Sugawara,[1] Fumiaki Sasaki,[3] Yukiko Tsunematsu,[3] Atsushi Kikuta,[3] Masahiro Fukuzawa,[3] Hajime Okita,[3] Jun-ichi Hata,[3] Hidenobu Soejima,[4] and Yasuhiko Kaneko[1,3*]

[1]Research Institute for Clinical Oncology, Saitama Cancer Center, Ina, Saitama, Japan
[2]Department of Pediatrics, Juntendo University Nerima Hospital, Tokyo, Japan
[3]Japan Wilms Tumor Study Group, Tokyo, Japan
[4]Department of Biomolecular Sciences, Saga University, Saga, Japan

We evaluated the *WT1* and *IGF2* status and performed chromosome and/or comparative genomic hybridization analysis in 43 tumor samples from patients with Wilms tumor. On this basis, we classified them into 4 groups: *WT1* abnormality, loss of heterozygosity (LOH) of *IGF2*, loss of imprinting (LOI) of *IGF2*, and retention of imprinting (ROI) of *IGF2*, which were seen in 12%, 30%, 16%, and 42% of the tumors, respectively. Patients in the LOI group were older than those in other groups ($P < 0.01$), and tumors in the *WT1* group had fewer cytogenetic changes than did those in the other groups ($P < 0.01$). It was found that 11q− and +12 were more frequent in the LOI group than in the *WT1*+LOH+ROI group ($P < 0.01$ and $P < 0.01$). There was no difference in the incidence of 16q− between the LOI group and the other groups; however, when we excluded 16 tumors with LOH on 11p15, 16q− tended to be more frequent in the LOI group than in the *WT1*+ROI group ($P = 0.06$). The association of 11q− or +12 with LOI of *IGF2* found in the present study suggests that many tumors with no *WT1* abnormalities need overexpression of *IGF2* together with biallelic inactivation of the tumor-suppressor gene on 11q and/or overexpression of growth-promoting genes on chromosome 12. The 11q gene may code for one of the proteins that constitute a CTCF insulator complex, and its mutation, deletion, or haploinsufficiency may cause insulator abnormalities that might lead to LOI of *IGF2*.

INTRODUCTION

Wilms tumor is the most common kidney tumor in childhood. A tumor-suppressor gene, *WT1*, was isolated in the 11p13 chromosomal region, but deletion or mutation has been found in only 15%–20% of Wilms tumors (Huff, 1998; Nakadate et al., 2001). Loss of imprinting (LOI) of insulin-like growth factor–II (*IGF2*), a paternally expressed gene at 11p15.5, has been reported to occur in 40%–70% of tumors (Ogawa et al., 1993; Rainier et al., 1993), and it was associated with a pathological subtype that occurs in a later stage of renal development (Ravenel et al., 2001). Several studies found the type of loss of heterozygosity (LOH) on 11p that is always caused by loss of the maternal chromosome in 30%–40% of tumors investigated (Schroeder et al., 1987; Grundy et al., 1994; Nakadate et al., 2001). LOI or LOH of *IGF2* may cause overexpression of a gene that gives tumor cells a growth advantage or modifies their differentiation stage (Sakatani et al., 2005), and *IGF2* is the primary candidate for being the *WT2* gene. Cytogenetic, comparative genomic hybridization (CGH), and LOH analyses of Wilms tumors showed gain or loss of specific chromosomes or chromosomal regions, indicating that *WT1*-wild-type tumors had more genomic alterations than *WT1*-mutant-type tumors (Nakadate et al., 1999; Hing et al., 2001; Ruteshouser et al., 2005). Furthermore, association of the long arm loss of chromosome 16 (16q−) with LOI of *IGF2* in Wilms tumor was recently reported (Mummert et al., 2005). However, 16q− was found in only a small portion of the tumors with LOI investigated, and no other cytogenetic abnormalities are known to be associated with LOI in the tumors. These studies indicate that Wilms tumor is a genetically heterogeneous disease, and further

Supported by: Grant-in-Aids for Third-Term Comprehensive 10-Year Strategy for Cancer Control and Scientific Research in the Ministry of Health, Labor, and Welfare of Japan.

*Correspondence to: Yasuhiko Kaneko, Division of Cancer Diagnosis, Research Institute for Clinical Oncology, Saitama Cancer Center, Ina, Saitama, Japan. E-mail: kaneko@cancer-c.pref.saitama.jp

Received 23 August 2005; Accepted 20 January 2006

DOI 10.1002/gcc.20321

Published online 3 March 2006 in Wiley InterScience (www.interscience.wiley.com).

studies are needed to clarify the genetic/epigenetic and cytogenetic background of the tumor.

We evaluated the *WT1* and *IGF2* status and performed chromosome and/or CGH analysis of 43 Wilms tumors, on the basis of which we classified them into 4 genetic/epigenetic groups: *WT1* abnormality, LOH of *IGF2*, LOI of *IGF2*, and retention of imprinting (ROI) of *IGF2*. We analyzed the relationship between cytogenetic and genetic/epigenetic changes and found an association of LOI of *IGF2* with 11q– and +12 and possibly also with 16q–.

MATERIALS AND METHODS

Patient Samples

Tumor samples were available from 68 Japanese infants or children ranging in age from 2 months to 8 years who underwent surgery or biopsy between August 1984 and February 2003. These samples were selected on the basis of tissue availability and were not gathered consecutively. Of the 68 patients, 21 were registered in the Japan Wilms Tumor Group Study (JWITS). Samples of normal tissue were obtained from either the peripheral blood or normal renal tissue adjacent to the tumor from the same patients. Informed consent was obtained from the parents, and the study design was approved by the ethics committee of Saitama Cancer Center. The tumors were staged according to the National Wilms' Tumor Study group (NWTS) staging system, and most patients were treated according to NWTS protocols (d'Angio et al., 1989). None of the 68 patients had a family history of Wilms tumor. One patient (275) had Drash syndrome, and another patient (953) had bilateral tumors; the remaining patients had sporadic and unilateral tumors (Table 1).

Histological Examination

In all tumors, the diagnosis of Wilms tumor was made with routine hematoxylin- and eosin-stained pathology slides by local pathologists from each institution according to the classification proposed by the Japanese Pathological Society and/or the NWTS pathology panel (Beckwith et al., 1978; Japanese Pathological Society, 1988). Twenty-one cases that were registered at the JWITS were also reviewed by the pathology panel.

Cytogenetic, Fluorescence In Situ Hybridization, and CGH Studies

Chromosomes from tumor cells were studied by methods reported previously (Nakadate et al., 1999), and karyotypes were described according to the International System of Human Cytogenetic Nomenclature (ISCN, 1995). Fluorescence in situ hybridization (FISH) using Vysis probes [CEP 3 (chromosome 3 centromere), CEP 12 (chromosome 12 centromere), CBFB (16q22), and MLL (11q23); Downers Grove, IL) were carried out as described previously (Watanabe et al., 2002). CEP 12 was used to detect trisomy 12 and CEP 3 was used as a control because chromosome and CGH analyses detected 2 copies of chromosome 3 in almost all Wilms tumors, and the CBFB and MLL probes were used to detect 16q– and 11q–, respectively. Karyotypes of 11 of the 43 tumors described in Table 1 were reported previously (Nakadate et al., 1999).

CGH analysis was performed as described previously (Kumon et al., 2000). A chromosomal region was considered overrepresented or underrepresented if the average ratio profile was above 1.25 or below 0.75, respectively.

Analyses of WT1 Abnormalities and Allelic Loss on 11p and 11q

DNA preparation and digestion and Southern blot analysis using a *WT1* cDNA probe (WT33; Call et al., 1990), PCR–single-strand conformation polymorphism (SSCP) and subsequent direct-sequencing analysis, and allelic loss analysis on 11p and 11q were performed as described previously (Nakadate et al., 2001). Whether there was allelic loss on 11p and 11q was determined by PCR using microsatellite markers of D11S922, *TH*, *IGF2*, D11S932, *PAX6*, D11S903, D11S4100, *NCAM*, D11S1885, D11S29, and D11S1364 and using the restriction fragment length polymorphism (RFLP) sites of *WT1* (Tadokoro et al., 1993). The primer sequences used for PCR were obtained from the Genome Database (http://www.gdb.org). The results of the allelic loss analysis on 11p and 11q for 21 of the 43 tumors described in Tables 1 and 2 were reported previously (Nakadate et al., 2001).

The results of the study of promoter hypermethylation of *WT1* were reported previously (Satoh et al., 2003).

Analysis of *IGF2* Allelic Expression and Loss

The *Apa*I/*Ava*II polymorphism site in exon 9 was used to evaluate allelic expression of *IGF2*. PCR with genomic DNA from normal tissue and identification of heterozygous specimens after *Ava*II and *Hin*fI digestion were performed as described previously (Watanabe et al., 2002). RT-PCR products from the tumor RNA also were

TABLE 1. Clinical, Genetic, Karyotypic and CGH findings in 43 Wilms Tumors

Patients number	Age/Sex	Stage of disease	*WT1* Abnormality	Karyotype	CGH	CEP 12/CEP 3	CBFB
Tumors with *WT1* abnormalities and LOH or ROI of *IGF2* (n = 5)							
275*	1 y 0 m/F	I	Mutation in exon 8	48,XX,+3,+6	ND		
832*	9 m/F	II	Mutation in exon 2	45,XX,del(3)(p12p14),−7	ND		
949*	1 y 3 m/F	II	Promoter methylation	44,X,-X,dic r(1;11)(p3?q3?;q25?p1?),inv(9)(p11q12)c	ND		
2375	1 y 9 m/M	IV	Homozygous deletion	46,XY	N		
M289	5 y 4 m/F	II	Mutation in exon 7	ND	enh(18),dim(11p13–11q12, 19,22)		
Tumors with LOH of *IGF2* and no *WT1* abnormalities (n = 13)							
325*	1 y 6 m/M	I	None	47,XY,+8,del(14)(q22)	ND		
528*	4 y 1 m/F	II	None	56,XX,+5,+7,+7,+9,+10,+12,+13,+18,+19,+22	enh(1q,4p,7,8,9,10,12,13,18)	3/2	2
575	3 y 11 m/M	II	None	46,XY	enh(1q)		
871	1 y 4 m/F	I	None	NM	N	2/2	2
918*	4 y 6 m/M	III	None	45,X,-Y	ND		
1075	2 y 4 m//M	IV	None	NM	N		
1390	4 y 0 m/M	I	None	NM	enh(Yq)		
1570*	11 m/F	II	None	51,XX,+7,+8,+10,+12,+13,?del(16)(q22)	enh(7,12,13),dim(16q22–qter)	3/2	1
1658*	2 y 8 m/M	III	None	46,XY,der(16)t(1;16)(q21;q12)	ND		
1752	1 y 0 m/F	III	None	46,XX	N		
2488	3 m/F	I	None	46,XX	N		
M134	10 m/F	II	None	ND	enh(6q),dim(7p)		
M204	3 y 9 m/F	IV	None	ND	enh(8,9,20),dim(Y)		
Tumors with LOI of *IGF2* and no *WT1* abnormalities (n = 7)							
548	3 y 1 m/M	II	None	NM	enh(6,8,9,12)		
1206*	3 y 10 m/F	II	None	50,XX,+12,inc/11q- detected by FISH (MLL)	ND	3/2	2
1207	4 y 4 m/F	III	None	76–87 complex changes	enh(12),dim(9,10p,11q,16q,18p)		
1435*	6 y 1 m/F	III	None	53,XX,+12,inc	ND	3/2	2
1535*	3 y 8 m/F	II	None	46,XX,dup(1)(q21q25),der(11)t(1;11)(q21;q22),del(16)(q22)	enh(1q,4p15–pter),dim(11q13–qter,16q)		
M269	4 y 6 m/F	IV	None	ND	enh(7q,14q21–qter),dim(7p,X)		
M291	8 y 0 m/F	I	None	ND	enh(1q,6,9p,12,13,18q),dim(1p,11q,19)		

(Continued)

TABLE 1. Clinical, Genetic, Karyotypic and CGH findings in 43 Wilms Tumors (Continued)

Patients number	Age/Sex	Stage of disease	*WT1* Abnormality	Karyotype	CGH	CEP 12/CEP 3	CBFB
Tumors with ROI of *IGF2* and no *WT1* abnormalities (n = 18)							
884	2 m/M	III	None	46,XY	N	2/2	2
953	1 y 1 m/F	V	None	47,XX,add(2)(p25), del(7)(q11q22),+8	ND		
1371	5 m/F	IV	None	NM	N		
1420	6 m/F	Unknown	None	46,XX	N		
1879	7 m/M	I	None	46,XY	N		
2011	2 y 7 m/M	II	None	55,XY,+2,+6,+7,+8, +10,+del(12)(q23) +del(12)(q23),+13,+14	enh(1q,2,6,7q21–qter,8,10, 12pter–q23,13,15), dim(1p,18p)		
2385	1 y 4 m/F	IV	None	46,XX	N		
2677	4 y 4 m/F	II	None	46,XX	enh(2)		
2749	5 y 2 m/M	II	None	46,XY	dim(22)		
M126	2 y 5 m/F	III	None	ND	enh(2p14–pter,3q,6,7,8, 12,13,17)		
M175	1 y 9 m/F	I	None	ND	N		
M188	1 y 0 m/M	I	None	ND	N		
M196	1 y 5 m/F	III	None	ND	N		
M232	1 y 2 m/F	II	None	ND	N		
M233	5 y 3 m/F	IV	None	ND	enh(6,8)		
M238	6 m/F	I	None	ND	enh(7,8,10,12,13,17,18)		
M258	4 m/M	I	None	ND	N		
M290	2 y 1 m/M	II	None	ND	enh(1q,6,7,9,12),dim(18p,Y)		

*Karyotypes of these tumors were reported previously (Nakadate et al., 1999).
Abbreviations: NM, no mitotic cells; ND, not done; N, normal; 3/2, 3 copies of CEP 12 and 2 copies of CEP 3 detected by FISH; 2, 2 copies of CBFB detected by FISH.

TABLE 2. Allelic Status of 11p and 11q and *IGF2* Imprinting Status in *WT1*, LOH of *IGF2*, and LOI of *IGF2* Wilms Tumor Groups

	11p15					11p13		11p11	11q21–22	11q23				*WT1* abnormality[a]	11q-detected by CGH/ cytogenetics
	S922	*IGF2*	*IGF2-LOI*	*TH01*	*S932*	*PAX6*	*WT1*	*S903*	*S4100*	*NCAM*	*S1855*	*S29*	*S1364*		
Tumors with *WT1* abnormalities and LOH, LOI, or ROI of *IGF2* ($n = 5$)															
275	—	●	—	●	●	—	●	—	—	○	—	○	—	Mutation in exon 8	Not detected
832	—	—	—	●	●	●	●	—	○	○	—	—	○	Mutation in exon 2	Not detected
949	—	—	—	●	—	—	●	●	●	—	—	—	●	Promoter methylation	Not detected
M289	—	○	□	○	○	○	●	●	—	—	○	○	○	Mutation in exon 7	Not detected
2375	○	○	□	○	○	—	▲	—	○	○	—	—	○	Homozygous deletion	Not detected
Tumors with LOH of *IGF* and no *WT1* abnormalities ($n = 13$)															
325	●	—	—	—	—	—	●	—	○	○	—	○	○	None	Not detected
528	—	●	—	●	●	●	—	—	●	—	●	—	●	None	Not detected
575	●	●	—	●	●	—	○	—	○	○	—	—	○	None	Not detected
871	●	—	—	●	—	●	—	—	—	○	○	○	○	None	Not detected
918	●	—	—	—	—	○	○	○	—	—	○	○	○	None	Not detected
1075	—	—	—	●	●	—	○	○	○	○	○	—	○	None	Not detected
1390	—	—	—	●	—	—	●	○	○	○	○	—	—	None	Not detected
1570	—	●	—	—	●	●	—	—	—	●	●	●	—	None	Not detected
1658	—	—	—	●	—	—	—	—	—	—	○	○	—	None	Not detected
1752	●	—	—	●	●	—	●	●	—	—	—	○	○	None	Not detected
2488	●	—	—	—	●	●	●	—	○	—	○	○	○	None	Not detected
M134	—	●	—	—	●	●	●	●	○	○	○	○	—	None	Not detected
M204	—	—	—	—	●	●	●	—	—	●	—	—	○	None	Not detected
Tumors with LOI of *IGF2* and no *WT1* abnormalities ($n = 7$)															
548	—	○	■	○	○	—	○	—	○	—	—	○	○	None	Not detected
1206	—	○	■	○	○	○	○	○	○	—	—	●	●	None	Detected
1207	—	○	■	○	—	—	—	○	—	—	—	—	●	None	Detected
1435	—	○	■	—	—	○	○	—	○	○	—	○	○	None	Not detected
1535	○	○	■	○	—	—	○	—	—	●	●	●	—	None	Detected
M269	○	○	■	○	○	○	○	○	○	—	—	○	○	None	Not detected
M291	○	—	■	○	—	○	○	—	●	—	●	●	●	None	Detected

[a]Details of *WT1* abnormality are described in the text.
● Loss of heterozygosity; ○ Retention of heterozygosity; — Not informative; ■ Loss of *IGF2* imprinting; □ Retention of *IGF2* imprinting; ▲ Homozygous *WT1* deletion.

digested with *Ava*II and *Hinf*I, and allelic expression of *IGF2* was determined.

Statistical Analysis

The significance of differences in various clinical and cytogenetic aspects of the disease among the 4 genetic/epigenetic groups of tumors was determined by the chi-square or Fisher's exact tests. Differences in the mean age of the patients and in the average number of chromosome changes between any 2 of the 4 groups were examined with Welch's *t* test.

RESULTS

Allelic Loss on 11p and 11q

Allelic loss on 11p and 11q was analyzed in Wilms tumor samples from 68 patients. Informative 11p15 loci were found in normal tissue from 64 of the patients; the 11p15 loci in the tissue from the other 4 patients were uninformative. Of the 64 informative tumors, 16 showed LOH. Of the 48 tumors without LOH, 27 were informative for the *Apa*I/*Ava*II polymorphism site of the *IGF2* gene. Thus, 43 tumor samples were the subject of the present study.

Three tumors (949, 528, and 1570) showed LOH for the entire chromosome 11; 1 tumor (M204) showed LOH on 11p15–11q23, retaining heterozygosity in the more distal 11q locus; 3 tumors (575, 918, and 1075) showed LOH limited to the 11p15 region; and 9 (275, 832, 325, 871, 1390, 1658, 1752, 2488, and M134) showed LOH limited to the 11p15–11p13 region (Table 2). Of the 27 tumors without LOH on 11p15, 1 (M289) showed

LOH limited to 11p13–11p11, and 4 (C1206, C1207, C1535, and M291) showed LOH on 11q (Table 2).

WT1 Abnormalities

Of the 9 tumors with LOH limited to the 11p15–11p13 region, 2 showed a *WT1* mutation; one (275) had a missense mutation in exon 8 (G to A conversion in nucleotide 1064; Haber et al., 1991), and the other (832) had a nonsense mutation (C to T conversion in nucleotide 550) in exon 2 (Table 2). Another tumor (C949) was found to have *WT1* promoter methylation, which was examined in 21 of the 43 tumors, of which only 1 showed the methylation (Satoh et al., 2003). This tumor had a ring chromosome containing chromosomes 1 and 11. Because the incidence of promoter methylation was quite low, and no other tumors showed a ring chromosome containing chromosome 11 and LOH for the entire chromosome 11, the other 22 tumors whose *WT1* promoter methylation status was not examined were assumed to be unmethylated.

Of 27 tumors without LOH on 11p15, 1 (M289) with LOH limited to the 11p13–11p11 region had a missense mutation in exon 7 (G to T conversion in nucleotide 895), and another (C2375) with retention of heterozygosity (ROH) for the entire chromosome 11 had homozygous deletion of the 6.6-kb fragment of *WT1*, detected by Southern blotting with a *WT1* cDNA probe and *Eco*RI digestion (Call et al., 1990; Table 2).

LOI of *IGF2*

Of the 27 tumors with ROH in 11p15 and the informative *Apa*I/*Ava*II polymorphism site of *IGF2*, 7 showed LOI of *IGF2* (Tables 1 and 2, Fig. 1). Of the 20 ROI tumors, 2 (M289 and C2375) showed *WT1* abnormalities as described before.

Four Groups of Tumors Classified by *WT1* and *IGF2* Status

We classified 43 Wilms tumors into 4 groups on the basis of major genetic abnormalities: *WT1* abnormality, LOH of *IGF2*, LOI of *IGF2*, and tumors without *WT1* or *IGF2* abnormalities. Three tumors with a *WT1* abnormality and LOH on 11p15–11p13 were included in the *WT1* group because *WT1* abnormalities are believed to have a stronger impact on tumorigenicity than LOH of *IGF2*. Thus, of the 43 tumors, 5 were classified into the *WT1* group, 13 into the LOH group, 7 into the LOI group, and 18 into the ROI group (Table 1).

CGH patterns and/or karyotypes were available for all 43 tumors (Table 1). Four tumors (528, 1206, 1435, and 1570) with a hyperdiploid karyotype (≥50 chromosomes) and trisomy 12 with or without other changes were also studied by FISH using the CEP 3, CEP 12, and CBFB probes. All 4 tumors were shown to have trisomy 12, and 1 was shown to have 16q–. One tumor (1206) was shown to have 11q– using FISH with the *MLL* probe.

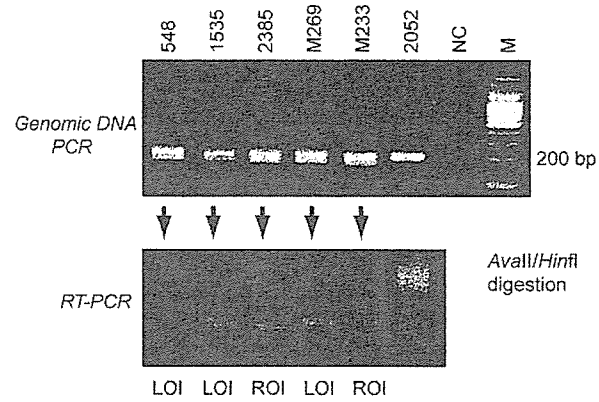

Figure 1. Electrophoretic patterns of products of genomic DNA PCR or reverse-transcription PCR after *Ava*II and *Hin*fI digestion. Normal tissue from samples 548, 1535, 2385, M269, and M233 was observed to have heterozygous *IGF2* alleles, and normal tissue from sample 2052 was observed to have homozygous *IGF2* alleles, in upper lanes; loss of imprinting was found in tumor tissue from samples 548, 1535, and M269 and retention of imprinting in tumor tissue from samples 2385 and M233, in lower lanes [NC, negative control (H_2O); M, size marker].

Clinical Characteristics of Patients in Each Tumor Group

The mean age of the patients was higher in the LOI group than in the *WT1* ($P = 0.03$), the LOH ($P = 0.01$), the ROI ($P < 0.01$), or the *WT1* + LOH + ROI ($P < 0.01$) groups (Table 3). There were no differences in stage distribution among the 4 groups. The tumors of 42 patients were classified as having a favorable histology, and the tumor of 1 patient (1390) was classified as having unfavorable histology (the diffuse anaplasia type). Of the 43 patients, 41 were alive with no evidence of disease at the last follow-up (November 30, 2004). Two patients had died: the patient who had the diffuse anaplasia–type tumor died of the disease, and the patient in the *WT1* group who had Drash syndrome (275) died of renal failure.

Association of Chromosome Abnormalities with *IGF2* and *WT1* Status

Ten chromosome/CGH abnormalities were seen in 4 or more tumors (Table 3). Loss limited to 11q was more frequent in the LOI group than in the *WT1* ($P = 0.08$), the LOH ($P < 0.01$), the ROI ($P < 0.01$), or the *WT1* + LOH + ROI ($P < 0.01$)

TABLE 3. Relationship between Cytogenetic Abnormalities with 4 Wilms Tumor Groups Classified by *WT1* or *IGF2* Status

Tumors classified by *WT1* and *IFG2* status	Number of tumors	Mean age of patients in months (range)	Mean number of cytogenetic changes	+1q	+6	+7/+7q	7p-	+8	+10	11q-[a]	+12[b]	+13	16q-[c]
A. Tumors with *WT1* abnormalities and LOH or ROI of *IGF2*	5	24.2 (9–64)	0.4	0	1	0	1	0	0	0	0	0	0
B. Tumors with LOH of *IGF2* and no *WT1* abnormalities	13	28.7 (3–54)	1.5	3	1	2	1	4	2	0	2	2	2
C. Tumors with LOI of *IGF2* and no *WT1* abnormalities	7	57.4 (37–96)	2.7	2	2	1	1	1	0	4	5	1	2
D. Tumors with ROI of *IGF2* and no *WT1* abnormalities	18	23.2 (2–63)	1.3	2	4	4	0	6	2	0	4	3	0

Mean age: C versus A, $P = 0.03$; C versus B, $P = 0.01$; C versus D, $P < 0.01$; C versus A+B+D, $P < 0.01$.
Mean number of cytogenetic changes: A versus B, $P = 0.12$; A versus C, $P < 0.01$; A versus D, $P = 0.13$; A versus B+C+D, $P < 0.01$.
[a]11q-: C versus A, $P = 0.08$; C versus B, $P < 0.01$; C versus D, $P < 0.01$; C versus A+B+D, $P < 0.01$; C versus A (2 tumors with ROI)+D, $P < 0.01$.
[b]+12: C versus A, $P = 0.03$; C versus B, $P = 0.02$; C versus D, $P = 0.06$; C versus A+B+D, $P < 0.01$; C versus A (2 tumors with ROI)+D, $P = 0.02$.
[c]16q-: C versus A, $P = 0.46$; C versus B, $P = 0.6$; C versus D, $P = 0.06$; C versus A+B+D, $P = 0.12$; C versus A (2 tumors with ROI)+D, $P = 0.06$.

groups. When we added 4 tumors with LOH in the entire chromosome 11 or in the 11p15–11q23 region to the 11q− category, 11q− was still more frequent in the LOI group than in the *WT1*+LOH+ROI group ($P = 0.02$).

Trisomy 12 was more frequent in the LOI group than in the *WT1* ($P = 0.03$), LOH ($P = 0.02$), ROI ($P = 0.06$), or LOH+ROI+*WT1* ($P < 0.01$) groups. Loss of 16q was found only in the LOI or the LOH group, but there was no significant difference among the 4 groups, or between the LOI and the *WT1*+LOH+ROI groups ($P = 0.12$). Mummert et al. (2005) excluded tumors with LOH on 11p15 in a correlation analysis of 16q− and LOI of *IGF2* because LOI of the maternal *IGF2* allele prior to its deletion could not be ascertained. When we excluded 16 tumors with LOH on 11p15, 16q− tended to be more frequent in the LOI group than in the *WT1* group with the ROI of *IGF2* + ROI group ($P = 0.06$). No other associations between chromosome abnormalities with any of the 4 groups were found (Fig. 2).

For the 10 chromosome/CGH abnormalities observed in 4 or more tumors, the mean number per tumor was lower in the *WT1* group (0.4/tumor) than in the LOH (1.5/tumor; $P = 0.12$), LOI (2.7/tumor; $P < 0.01$), ROI (1.3/tumor; $P = 0.13$), or LOH+LOI+ROI (1.7/tumor; $P < 0.01$) groups (Table 3).

DISCUSSION

Wilms tumor is a heterogeneous disease showing various genetic/epigenetic abnormalities, including mutations/deletions of the *WT1* gene, LOH or LOI of the *IGF2* gene, and *CTNNB1* mutations frequently associated with *WT1* abnormalities (Ogawa et al., 1993; Rainier et al., 1993; Koesters et al., 1999; Mati et al., 2000; Ravenel et al., 2001). In addition, we previously reported that hyperdiploid tumors, usually including trisomy 12, might be a unique subgroup of tumors with no *WT1* abnormalities (Nakadate et al., 1999). Cytogenetic, CGH, and LOH studies have found recurrent abnormalities, including gains of 1q, 2, 6, 7, 8, 10, 12, 13, and 18 and losses of 1p, 7p, 9q, 11p, 11q, 16q, and 22q (Nakadate et al., 1999; Hing et al., 2001; Ruteshouser et al., 2005). None of the previous studies simultaneously examined the status of *WT1*, LOH or LOI of *IGF2*, LOH on 11p and 11q, and all chromosome/CGH patterns. The present study showed *WT1* abnormalities, LOH of *IGF2*, LOI of *IGF2*, and ROI of *IGF2* in 12%, 30%, 16%, and 42%, respectively, of 43 Wilms tumors.

Recently, Mummert et al. (2005) reported that Wilms tumors with 16q− had expression of *CTCF* half that of expression in tumors with normal chromosomes 16 and that LOI of *IGF2* was associated with loss of 16q. The *CTCF* gene, at 16q22, codes for an insulator protein. According to Mummert et al. (2005), when less CTCF was available to bind the differentially methylated region (DMR) upstream of *H19*, access of maternal *IGF2* to an enhancer downstream of *H19* might occur. The present study confirmed that tumors with 16q− showed either LOI or LOH of *IGF2* (Yeh et al., 2002; Mummert et al., 2005) and provided support for the association of 16q− with LOI of *IGF2*. Furthermore, the present study disclosed that 11q− and +12 were more frequent in tumors with LOI than in those with LOH, ROI, or *WT1* abnormalities.

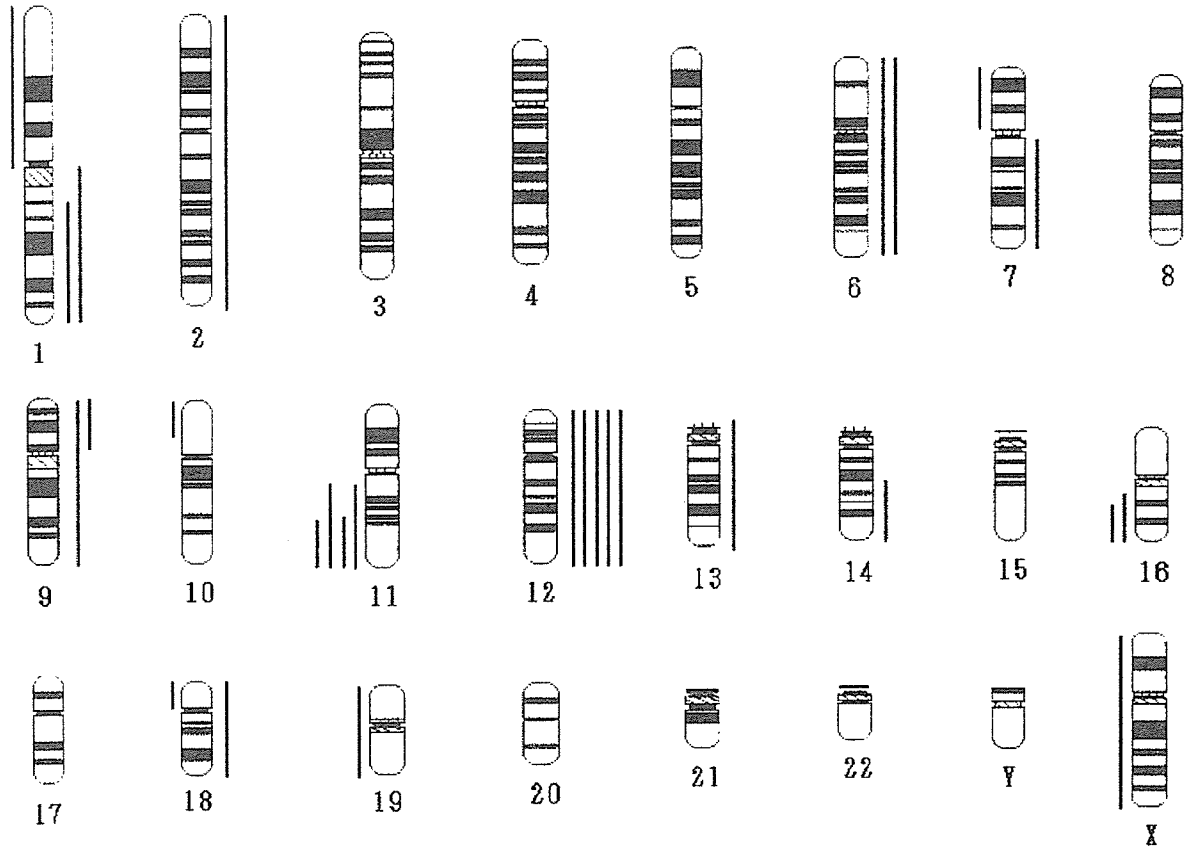

Figure 2. Summary of chromosome changes in the LOI group detected by CGH, chromosome, FISH, and/or LOH analyses. Gains and losses are shown on the right and left sides, respectively.

Overexpression of *IGF2* can be caused by LOI or by duplication of the paternal chromosome 11 with loss of the maternal chromosome 11 (LOH). LOI or LOH of *IGF2* has been detected in various embryonal tumors, including Wilms tumor, rhabdomyosarcoma, and hepatoblastoma (Ogawa et al., 1993; Rainier et al., 1993, 1995; Zhan et al., 1994). More recently, microdeletion of the maternal *H19* DMR was reported in a large family of people with Beckwith–Wiedemann syndrome (Prawitt et al., 2005). Although LOI of *IGF2* was found in fibroblasts from all 4 individuals with the microdeletion, 3 with a second genetic lesion (duplication of the microdeleted maternal *IGF2* locus), but not the one without it, developed Beckwith–Wiedemann syndrome and Wilms tumor. These findings suggest that LOI of *IGF2* or duplication of the paternal *IGF2* may be one of several genetic and epigenetic events that promote tumor cell proliferation.

The present study found an association of 11q– with LOI of *IGF2*. Very recently, Yuan et al. (2005) studied LOI of *IGF2* by assessing DNA methylation of the *H19* DMR and LOH by single-nucleotide polymorphism (SNP) chips in 58 sporadic Wilms tumors, 22 of which showed LOI. Partial loss of 11q and loss of whole chromosome 11 were found in 6 and 0, respectively, of the 22 LOI tumors, and in 1 and 13, respectively, of the 36 non-LOI tumors. They stated that 11q– was not associated with LOI. When we added 4 tumors with LOH for the entire chromosome 11 or the 11p and 11q regions into the 11q– category in the present series, 11q– was still more frequent in the LOI group than in the *WT1* + LOH + ROI group. Whole loss of chromosome 11 may play a role in loss of the wild-type *WT1* allele or in loss of the maternal *IGF2* allele, and 11q– may be a bystander in tumors with whole loss of chromosome 11 and *WT1* mutation or duplication of the paternal *IGF2* (LOH). When the 13 tumors with loss of the entire chromosome 11 from the series reported by Yuan et al. (2005) were excluded, partial loss of 11q was more frequent in the LOI tumors (6 of 22 tumors) than in the non-LOI tumors (1 of 23 tumors), $P < 0.01$, Fisher's exact

test. Thus, the present study and that of Yuan et al. (2005) lead to the same conclusion: chromosomal loss limited to 11q is associated with LOI of *IGF2* in Wilms tumor.

It has been hypothesized that 11q harbors a tumor-suppressor gene involved in the development of Wilms tumor (Radice et al., 1995; Nakadate et al., 2001). The association between 11q− and LOI of *IGF2* found in the present study suggests that Wilms tumors with overexpression of *IGF2* require deletion/mutation of the putative 11q gene in order to develop to full-blown tumors. As we have shown (Tables 1 and 2, Fig. 2), the present CGH and cytogenetic study detected physical loss of 11q DNA, rather than mitotic recombination, in the 4 tumors with LOI and 11q LOH. The gene on 11q may code for one of the proteins that constitute a CTCF insulator complex, and mutation, deletion, or haploinsufficiency of the gene may cause insulator abnormalities that might lead to LOI of *IGF2* (Ohlsson et al., 2001).

The present study also found an association between trisomy 12 and LOI of *IGF2*. We previously proposed that hyperdiploid tumors (≥50 chromosomes) make up a unique subgroup of Wilms tumors characterized by the absence of *WT1* abnormalities and nonrandom gains of chromosomes, usually including trisomy 12 (Nakadate et al., 1999). The present study added another characteristic, namely, the tendency to show LOI of *IGF2*, to the list of characteristics of hyperdiploid tumors. *CCND2* and *CDK4*, which are growth-promoting genes on chromosome 12, are overexpressed in Wilms tumors (Faussillon et al., 2005), and it is speculated that tumors with LOI of *IGF2* also need trisomy 12 in order to proliferate in an accelerated manner.

Ravenel et al. (2001) reported that patients who had Wilms tumors with LOI of *IGF2* were older than those who had tumors with normal imprinting and that the tumors with LOI were more likely to be of a pathological subtype associated with a later stage of renal development. The present study confirmed that patients with tumors with LOI were older than those who had tumors of other subtypes. Chromosome changes were most frequent in the LOI group and least frequent in the *WT1* group (Table 3). We suggest from the findings described above that tumors with LOI need far more genetic events to develop into full-blown tumors than do those with certain genetic types of tumors; it will take time to accumulate the genetic and epigenetic events that might explain why patients with LOI of *IGF2* are older.

ACKNOWLEDGMENTS

We are grateful to Dr. T. Hirama, Hokkaido Children's Medical Center (Otaru, Hokkaido); Dr. H. Mugishima, Nihon University (Itabashi-Ku, Tokyo); Dr. S. Koizumi, Kanazawa University (Kanazawa, Ishikawa); H. Kigasawa, Kanagawa Children's Medical Center (Yokahama, Kanagawa); Y. Horikoshi, Shizuoka Children's Hospital (Shizuoka, Shizuoka); T. Matsubayashi, Seirei Hamamatsu Hospital (Hamamatsu, Shizuoka); Dr. K. Kato, Nagoya First Red Cross Hospital (Nagoya, Aichi), Dr. S. Ohta, Shiga Medical College (Ohtsu, Shiga); Dr. M. Miyake, Osaka Medical College (Takatsuki, Osaka); and Dr. Y. Ishida, Ehime University (Shigenobu, Ehime) for providing samples and clinical data.

REFERENCES

Beckwith JB, Palmer NF. 1978. Histopathology and prognosis of Wilms tumor: results from the First National Wilms' Tumor Study. Cancer 41:1937–1948.

Call KM, Glaser T, Ito CY, Buckler AJ, Pelletier J, Haber DA, Rose EA, Kral A, Yeger H, Lewis WH, Jones C, Housman DE. 1990. Isolation and characterization of a zinc finger polypeptide gene at the human chromosome 11 Wilms' tumor locus. Cell 60:509–520.

D'Angio GJ, Breslow N, Beckwith JB, Evans A, Baum H, deLorimier A, Fernbach D, Hrabovsky E, Jones B, Kelalis P, Othersen B, Tefft M, Thomas PRM. 1989. Treatment of Wilms' tumor. Results of the Third National Wilms' Tumor Study. Cancer 64:349–360.

Faussillon M, Monnier L, Junien C, Jeanpierre C. 2005. Frequent overexpression of cyclin D2/cyclin-dependent kinase 4 in Wilms' tumor. Cancer Lett 221:67–75.

Grundy PE, Telzerow PE, Breslow N, Moksness J, Huff V, Paterson MC. 1994. Loss of heterozygosity for chromosomes 16q and 1p in Wilms' tumors predicts an adverse outcome. Cancer Res 54:2331–2333.

Japanese Pathological Society. 1988. Committee on histological classification of childhood tumors: tumors of the urinary system. Kanahara Shuppan, Tokyo.

Haber DA, Sohn RL, Buckler AJ, Pelletier J, Call KM, Housman DE. 1991. Alternative splicing and genomic structure of the Wilms tumor gene WT1. Proc Nat Acad Sci USA 88:9618–9622.

Hing S, Lu YJ, Summersgill B, King-Underwood L, Nicholson J, Grundy P, Grundy R, Gessler M, Shipley J, Pritchard-Jones K. 2001. Gain of 1q is associated with adverse outcome in favorable histology Wilms' tumors. Am J Pathol 158:393–398.

Huff V. 1998. Wilms tumor genetics. Am J Med Genet 79:260–267.

Koesters R, Ridder R, Kopp-Schneider A, Betts D, Adams V, Niggli F, Briner J. 1999. Mutational activation of the beta-catenin proto-oncogene is a common event in the development of Wilms' tumors. Cancer Res 59:3880–3882.

Kumon K, Kobayashi H, Namiki T, Tsunematsu Y, Miyauchi J, Kikuta A, Horikoshi Y, Komada Y, Hatae Y, Eguchi H, Kaneko Y. 2001. Frequent increase of DNA copy number in the 2q24 chromosomal region and its association with a poor clinical outcome in hepatoblastoma: cytogenetic and comparative genomic hybridization analysis. Jpn J Cancer Res 92:854–862.

Maiti S, Alam R, Amos CI, Huff V. 2000. Frequent association of beta-catenin and WT1 mutations in Wilms tumors. Cancer Res 60:6288–6292.

Mummert SK, Lobanenkov VA, Feinberg AP. 2005. Association of chromosome arm 16q loss with loss of imprinting of insulin-like growth factor–II in Wilms tumor. Genes Chromosomes Cancer 43:155–161.

Nakadate H, Tsuchiya T, Maseki N, Hatae Y, Tsunematsu Y, Horikoshi Y, Ishida Y, Kikuta A, Eguchi H, Endo M, Miyake M, Sakurai M, Kaneko Y. 1999. Correlation of chromosome abnormalities with presence or absence of WT1 deletions/mutations in Wilms tumor. Genes Chromosomes Cancer 25:26–32.

Nakadate H, Yokomori K, Watanabe N, Tsuchiya T, Namiki T, Kobayshi H, Suita S, Tsunematsu Y, Horikoshi Y, Hatae Y, Endo M, Komada Y, Eguchi H, Toyoda Y, Kikuta A, Kobayashi R, Kaneko Y. 2001. Mutations/deletions of the WT1 gene, loss of heterozygosity on chromosome arms 11p and 11q, chromosome ploidy and histology in Wilms' tumors in Japan. Int J Cancer 94:396–400.

Ogawa O, Eccles MR, Szeto J, McNoe LA, Yun K, Maw MA, Smith PJ, Reeve AE. 1993. Relaxation of insulin-like growth factor II gene imprinting implicated in Wilms' tumour. Nature 62:749–751.

Ohlsson R, Renkawitz R, Lobanenkov V. 2001. CTCF is a uniquely versatile transcription regulator linked to epigenetics and disease. Trends Genet 17:520–527.

Prawitt D, Enklaar T, Gartner-Rupprecht B, Spangenberg C, Oswald M, Lausch E, Schmidtke P, Reutzel D, Fees S, Lucito R, Korzon M, Brozek I, Limon J, Housman DE, Pelletier J, Zabel B. 2005. Microdeletion of target sites for insulator protein CTCF in a chromosome 11p15 imprinting center in Beckwith–Wiedemann syndrome and Wilms' tumor. Proc Natl Acad Sci USA 102:4085–4090.

Radice P, Perotti D, De Benedetti V, Mondini P, Radice MT, Pilotti S, Luksch R, Fossati Bellani F, Pierotti MA. 1995. Allelotyping in Wilms tumors identifies a putative third tumor suppressor gene on chromosome 11. Genomics 27:497–501.

Rainier S, Dobry CJ, Feinberg AP. 1995. Loss of imprinting in hepatoblastoma. Cancer Res 55:1836–1838.

Rainier S, Johnson LA, Dobry CJ, Ping AJ, Grundy PE, Feinberg AP. 1993. Relaxation of imprint genes in human cancer. Nature 362:747–749.

Ravenel JD, Broman KW, Perlman EJ, Niemitz EL, Jayawardena TM, Bell DW, Haber DA, Uejima H, Feinberg AP. 2001. Loss of imprinting of insulin-like growth factor–II (IGF2) gene in distinguishing specific biologic subtypes of Wilms tumor. J Natl Cancer Inst 93:1698–1703.

Ruteshouser EC, Hendrickson BW, Colella S, Krahe R, Pinto L, Huff V. 2005. Genome–wide loss of heterozygosity analysis of WT1-wild-type and WT1-mutant Wilms tumors. Genes Chromosomes Cancer 43:172–180.

Sakatani T, Kaneda A, Iacobuzio-Donahue CA, Carter MG, de Boom Witzel S, Okano H, Ko MS, Ohlsson R, Longo DL, Feinberg AP. 2005. Loss of imprinting of Igf2 alters intestinal maturation and tumorigenesis in mice. Science 307:1976–1978.

Satoh Y, Nakagawachi T, Nakadate H, Kaneko Y, Masaki Z, Mukai T, Soejima H. 2003. Significant reduction of WT1 gene expression, possibly due to epigenetic alteration in Wilms' tumor. J Biochem 133:303–308.

Schroeder WT, Chao LY, Dao DD, Strong LC, Pathak S, Riccardi V, Lewis WH, Saunders GF. 1987. Nonrandom loss of maternal chromosome 11 alleles in Wilms tumors. Am J Hum Genet 40:413–420.

Tadokoro K, Oki N, Sakai A, Fujii H, Ohshima A, Nagafuchi S, Inoue T, Yamada M. PCR detection of 9 polymorphisms in the WT1 gene. 1993. Hum Mol Genet 2:2205–2206.

Watanabe N, Kobayashi H, Hirama T, Kikuta A, Koizumi S, Tsuru T, Kaneko Y. 2002. Cryptic t(12;15)(p13;q26) producing the ETV6–NTRK3 fusion gene and no loss of IGF2 imprinting in congenital mesoblastic nephroma with trisomy 11: fluorescence in situ hybridization and IGF2 allelic expression analysis. Cancer Genet Cytogenet 136:10–16.

Yeh A, Wei M, Golub SB, Yamashiro DJ, Murty VV, Tycko B. 2002. Chromosome arm 16q in Wilms tumors: unbalanced chromosomal translocations, loss of heterozygosity, and assessment of the CTCF gene. Genes Chromosomes Cancer 35:156–163.

Yuan E, Li CM, Yamashiro DJ, Kandel J, Thacker H, Murty VV, Tycko B. 2005. Genomic profiling maps loss of heterozygosity and defines the timing and stage dependence of epigenetic and genetic events in Wilms' tumors. Mol Cancer Res 3:493–502.

Radiotherapy and Oncology 80 (2006) 93–97
www.thegreenjournal.com

Treatment of lung damage

Retrospective analysis of steroid therapy for radiation-induced lung injury in lung cancer patients

Ikuo Sekine[a,*], Minako Sumi[b], Yoshinori Ito[b], Hiroshi Nokihara[a], Noboru Yamamoto[a], Hideo Kunitoh[a], Yuichiro Ohe[a], Tetsuro Kodama[a], Nagahiro Saijo[a], Tomohide Tamura[a]

[a]*Division of Internal Medicine and Thoracic Oncology, and* [b]*Division of Radiation Oncology, National Cancer Center Hospital, Tokyo, Japan*

Abstract

Purpose: To disclose characteristics of lung cancer patients developing radiation-induced lung injury treated with or without corticosteroid therapy.

Methods and materials: Radiographic changes, symptoms, history of corticosteroid prescription, and clinical course after 50–70 Gy of thoracic radiotherapy were retrospectively evaluated in 385 lung cancer patients.

Results: Radiation-induced lung injury was stable without corticosteroid in 307 patients (Group 1), stable with corticosteroid in 64 patients (Group 2), and progressive to death despite corticosteroid in 14 patients (Group 3). Fever and dyspnea were noted in 11%, 50% and 86% ($p < 0.001$), and in 13%, 44% and 57% ($p < 0.001$) patients in Groups 1–3, respectively. Median weeks between the end of radiotherapy and the first radiographic change were 9.9, 6.7 and 2.4 for Groups 1–3, respectively ($p < 0.001$). The initial prednisolone equivalent dose was 30–40 mg daily in 52 (67%) patients. A total of 16 (4.2%) patients died of radiation pneumonitis or steroid complication with a median survival of 45 (range, 8–107) days.

Conclusion: Development of fever and dyspnea, and short interval between the end of radiotherapy and the first radiographic change were associated with fatal radiation-induced lung injury. Prednisolone 30–40 mg daily was selected for the treatment in many patients.

Keywords: Radiation pneumonitis; Radiotherapy; Lung cancer; Corticosteroid

Thoracic radiotherapy is widely used for the curative and palliative treatment of lung cancer. Radiation-induced lung injury was first described as early as 1922 [1,2], and two types of lung injury, radiation pneumonitis and radiation fibrosis, were recognized in 1925 [3]. Radiation pneumonitis occurs in 5–15% of patients who have received radiation therapy for lung cancer. Its clinical symptoms are characterized by cough, dyspnea and fever developing between 1 and 3 months after the end of radiotherapy. Distinctive radiographic changes of radiation pneumonitis are a ground-glass opacification or diffuse haziness in early phase, and then alveolar infiltrates or dense consolidation in late phase in the region corresponding to the irradiated area [4–7]. Radiation pneumonitis may persist for a month or more and subside gradually. In severe cases, however, pneumonitis progresses to death due to respiratory failure within few weeks [4].

Use of adrenocorticotropic hormone (ACTH) and cortisone for radiation pneumonitis in a case was first reported in 1951 [8], and 9 cases of radiation pneumonitis treated with cortisone therapy in the literature were reviewed in 1968 [9]. Although no case series or clinical trials of corticosteroid therapy have been reported since that time, prednisolone has been given in patients with severe pneumonitis in clinical practice. The initial dose of prednisolone, approximately 30–100 mg daily, and very slow tapering schedule are in agreement among experts [4–6,10], because early withdrawal results in aggravation of pneumonitis [11–13]. There is no consensus, however, about criteria to define when steroids are required for radiation-induced lung injury. The objective of this study is to disclose general characteristics of lung cancer patients developing radiation-induced lung injury treated with or without corticosteroid therapy, to obtain data on the initiation criteria, dose, and taper schedule of corticosteroid therapy for further prospective trials.

Patients and methods

Consecutive lung cancer patients treated with thoracic radiotherapy at a total dose of 50–70 Gy in National Cancer

0167-8140/$ - see front matter doi:10.1016/j.radonc.2006.06.007

Center Hospital between January 1998 and December 2003 were subjects of this study. We retrospectively reviewed all chest X-ray films taken during 6 month period from the end of thoracic radiation to identify the first radiographic change and its progress. History of corticosteroid prescription, symptoms at the time of and one-month period after the first radiographic change in a chest X-ray film, and clinical course of radiation-induced lung injury were obtained from medical charts. The diagnosis of radiation-induced lung injury was defined as radiographic changes including opacification, diffuse haziness, infiltrates or consolidation conforming to the outline of the sharply demarcated irradiated area in a chest X-ray film. During clinical course, scarring (fibrosis) was developed within the irradiated area leading to a reduction in lung volume. In contrast, pulmonary infection spreads through anatomical structure of the lung, and the boundary of infiltrates corresponds to anatomical boundary of the lung. For patients with fever, the radiographical response to antibiotics was also evaluated. Observed differences in the proportions of patients in various patient subgroups were evaluated using Chi-square test. Differences between continuous variables were compared using Mann–Whitney tests. The Dr. SPSS II 11.0 for Windows software package (SPSS Japan Inc., Tokyo, Japan) was used for all statistical analyses.

Results

Of 544 lung cancer patients receiving thoracic radiotherapy at a total dose of 50–70 Gy, 111 patients were excluded from this study because they were not evaluable: loss of follow-up in 88 patients, early lung cancer progression in 18 patients, chemotherapy-induced neutropenic fever and pneumonia in three patients, death of bleeding from the esophageal stent in one patient, and no chest X-ray films available in one patient. In addition, 48 patients (11% of 433 evaluable patients) were also excluded because no radiation-induced lung injury was noted. Thus, the subject of this study was 385 patients.

Of the 385 patients, 78 (20%) received corticosteroid therapy for radiation-induced lung injury, and 307 did not. Radiation-induced lung injury was stable without corticosteroid in the 307 (80%) patients (Group 1), stable or in remission with corticosteroid in 64 (17%) patients (Group 2), and progressive to death despite corticosteroid in 14 (4%) patients (Group 3). No difference in sex, total dose, intent of radiotherapy, and combination chemotherapy was noted among three Groups, but median age of patients was higher in Group 3 (Table 1). Fever was developed in 50% of patients in Group 3 at the initial radiographic change, and in 86% of them during subsequent clinical course, while it was developed in only 11–12% of patients in Group 1 through their clinical course (Table 2). Dyspnea was developed in 57% of patients in Group 3 and in 44% of patients in Group 2 during clinical course, while it was developed in only 14% of patients in Group 1 (Table 2). A total of 88 patients developed fever at the initial change in chest X-ray and/or during subsequent clinical course. Of these, 43 patients received antibiotics, but no radiographical response was obtained in these patients. Five (2%) and seven (2%) patients in Group 1 developed bloody sputum and chest pain, respectively, but none in Group 2 or 3 developed these symptoms. The average interval of chest X-rays taken between the start of radiotherapy and the first appearance of radiographic change was 1.7 weeks for group 1, 1.3 weeks for group 2, and 0.9 weeks for group 3 ($P < 0.001$, Table 3). Interval between the end of radiotherapy and the first change in a chest X-ray was shorter in Group 3 than in Group 2 or Group 1 (Table 3). Of 57 patients in whom the first radiographic change was noted within three weeks, 9 (16%) died of pneumonitis, while radiation-induced lung injury that occurred 10 weeks or later after the end of radiation was easily managed with or without steroid therapy (Table 3). Oxygen content in the blood at the start of steroid therapy was examined in 70 patients of Groups 2 and 3. Oxygen content

Table 1
Patient demographics and radiotherapy performance

Characteristics	Total *N* (%)	Group 1	Group 2	Group 3	*p*-value
		N (%)	*N* (%)	*N* (%)	
Total	385 (100)	307 (80)	64 (17)	14 (4)	
Sex					
Male	300 (78)	240 (78)	47 (73)	13 (93)	0.28
Female	85 (22)	67 (22)	17 (27)	1 (7)	
Age median (range)	65 (28–87)	63 (28–87)	65 (37–83)	71 (65–84)	0.008
Total dose (Gy)					
Median (range)	60 (50–70)	60 (50–70)	60 (50–61)	60 (50–60)	0.50
Intent of radiotherapy					
Curative	298 (77)	232 (76)	52 (81)	14 (100)	0.074
Palliative	87 (23)	75 (24)	12 (19)	0 (0)	
Chemotherapy					
None	121 (31)	101 (33)	15 (23)	5 (36)	0.48
Sequential	121 (31)	93 (30)	25 (39)	3 (21)	
Concurrent	143 (37)	113 (37)	24 (38)	6 (43)	

Table 2
Symptoms through clinical courses

Symptom	At the initial change in chest X-ray				During subsequent clinical course			
	Group 1	Group 2	Group 3	p	Group 1[a]	Group 2[b]	Group3[b]	p
Cough	96 (31)	35 (56)	5 (36)	0.001	85 (28)	38 (59)	5 (36)	<0.001
Sputum	32 (10)	11 (18)	4 (29)	0.049	30 (10)	11 (17)	3 (21)	0.12
Hemosputum	5 (2)	0 (0)	0 (0)	0.53	4 (1)	0 (0)	0 (0)	0.60
Chest pain	7 (2)	0 (0)	0 (0)	0.40	2 (0.6)	0 (0)	0 (0)	0.78
Fever								
None	269 (88)	35 (56)	7 (50)	<0.001	272 (89)	32 (50)	2 (14)	<0.001
37.0–37.9 °C	18 (6)	11 (18)	2 (14)	24 (8)	16 (25)	5 (35)		
38 °C⩽	13 (4)	14 (22)	5 (36)	8 (3)	13 (20)	7 (50)		
Not specified	7 (2)	3 (4)	0 (0)	3 (1)	3 (4)	0 (0)		
Dyspnea	43 (14)	14 (22)	6 (43)	0.007	40 (13)	28 (44)	8 (57)	<0.001
Fever or dyspnea	75 (24)	37 (58)	10 (71)	<0.001	65 (21)	49 (77)	14 (100)	<0.001
Any	150 (49)	51 (81)	13 (93)	<0.001	118 (38)	60 (94)	14 (100)	<0.001

[a] During one month period following the initial change in the chest X-ray.
[b] At the start of steroid therapy.

Table 3
The chest X-ray intervals and first radiographic change

Weeks	Group 1	Group 2	Group 3	p-value
The average interval of chest X-rays (weeks)[a]				
Median (range)	1.7 (0.7 to 6.0)	1.3 (0.5 to 4.4)	0.9 (0.5 to 3.8)	<0.001
Duration between the end of radiotherapy and the first radiographic change (weeks)				
Median (range)	9.9 (−2.9 to 45.1)	6.7 (0 to 24.9)	2.4 (0.4 to 10.1)	<0.001
<6	82 (27)	26 (41)	11 (79)	<0.001
6–11.9	116 (38)	29 (45)	3 (21)	
12–17.9	71 (23)	7 (11)	0 (0)	
18⩽	38 (12)	2 (3)	0 (0)	

[a] Calculated as follows: the average interval of chest X-rays = (the first radiographic change − the start of radiotherapy)/the number of chest X-rays taken during this period/7).

was slightly decreased (PaO2 = 70–74.9 Torr) in 12 (19%) patients of Group 2 and one (7%) patient of Group 3, and moderately to severely decreased (PaO2 ⩽ 69.9 Torr or SpO2 ⩽ 92%) in 21 (33%) patients of Group 2 and 7 (50%) patients of Group 3 ($p = 0.38$).

Prednisolone was administered as the initial therapy in 69 (88%) patients of Groups 2 and 3. The initial prednisolone equivalent dose of steroid was 30–40 mg daily in 52 (67%), and 60 mg of higher only in 8 (10%) patients (Table 4). The median duration of the initial dose was 10 (range, 2–64) days, and the dose was reduced within 14 days in 57 (77%) patients. The median duration of steroid therapy was 10 (range, 2–28) weeks (Table 4). Steroid pulse therapy (methylprednisolone 1000 mg daily for three days) was administered as the initial therapy in one patient, and as salvage therapy in six patients at the time of pneumonitis aggravation. Among the seven patients, six died of respiratory failure due to progressive radiation pneumonitis.

Outcome of steroid therapy was evaluated in 76 patients (Fig. 1). Symptomatic relief was obtained and the steroid dose was reduced in 71 (93%) of the 76 patients, while no effect was noted in the remaining five patients, who all died of radiation pneumonitis despite escalated steroid administration. Of the 71 patients, 15 (21%) developed recurrent symptoms at the median daily prednisolone dose of 20 mg (range, 10–40 mg) within median 33 days (range, 21–42 days) from the start of the steroid therapy, and required steroids to be escalated. Of the 15 patients, nine died of radiation pneumonitis and one died of complication of steroid therapy. A total of 54 (71%) patients were in remission from pneumonitis and steroid therapy was terminated. The remainder 22 patients died during steroid therapy, 14 of radiation pneumonitis, two of infectious complication (bacterial pneumonia in one, and lung aspergillosis in another patient), five of lung cancer progression, and one of hemoptysis. Thus, 16 patients, who accounted for 4.2% of 385 patients receiving 50–70 Gy of thoracic radiotherapy, and who accounted for 21% of 78 patients treated with steroid therapy, died of radiation pneumonitis or complication associated with steroid therapy. Median survival from the start of steroid therapy in these patients was 45 (range, 8–107) days.

Discussion

Patients with radiation-induced lung injury have been managed in compliance with the expert opinions, because there has been no case series or clinical trial report on clinical course and corticosteroid use for this lung injury. This

Table 4
Corticosteroid, dose and duration of steroid therapy

	N (%)
Corticosteroid	
Prednisolone	69 (88)
Dexamethasone	4 (5)
Betamethasone	4 (5)
Methylprednisolone	1 (1)
Initial dose, mg/body daily (prednisolone equivalent)	
Pulse therapy	1 (1)
60	7 (9)
50	1 (1)
40	10 (13)
30	42 (54)
10–25	17 (22)
Duration of the initial dose, days	
Median (range)	10 (2–64)
⩽14	57 (77)
15–28	9 (12)
29⩽	8 (11)
Not evaluable	4
Total duration of steroid therapy, weeks	
Median (range)	10 (2–28)
⩽6	16 (30)
6.1–12	19 (35)
12.1–18	14 (26)
18.1⩽	5 (9)
Not evaluable	24

study is the first systemic review of these patients both who received corticosteroid therapy and who did not. Comparison between the expert opinions and the results of this study is given below. First, radiation-induced lung injury is severer when a radiographic change appears earlier [5]. In this study, the initial change in a chest X-ray film was observed in 9.9 (range, −3 to 45) weeks in Group 1, in 6.7 (range, 0–25) weeks in Group 2, and 2.4 (range, 0–10) weeks in Group 3 after the end of thoracic radiotherapy. If patients present with symptoms, presumably they receive a chest X-ray. Thus, the patients with symptoms may have radiographic findings seen sooner, since they receive an X-ray when they complain of symptoms. The average interval of chest X-rays taken between the start of radiotherapy and the first appearance of radiographic change was longer in Group 1 than that in groups 2 and 3. The difference, however, was negligibly small when compared with the difference in duration between the end of radiotherapy and the first radiographic change. Second, steroid administration is determined generally based on the severity of symptoms [5]. In this study steroid was used when patients developed dyspnea or fever. Dyspnea has been thought to be the cardinal symptom of radiation pneumonitis but fever to be unusual [5,10]. In this study, however, fever was highly associated with fatal radiation pneumonitis; fever was noted in 12% patients of Group 1, in 58% patients of Group 2, and 86% patients of Group 3. This study failed to show utility of blood gas analysis. An oxygen content in the blood was decreased moderately to severely in only 28 (36%) patients in Groups 2 and 3, and did not differ between the two groups. The oxygen content in Group 1 was measured in only small number of patients, and therefore it was not evaluable in this study. Third, 30–100 mg/day of prednisolone has been recommended as the initial dose [4–6,10]. In our practice, a dose of 30–40 mg was the most frequently used. We selected this relatively low dose of steroid mostly because steroid therapy was started in out patient clinic. Forth, duration of the initial dose was within two weeks in 73% of patients, which is consistent to most expert opinions [6,10]. In contrast, tapering schedules varied between a pa-

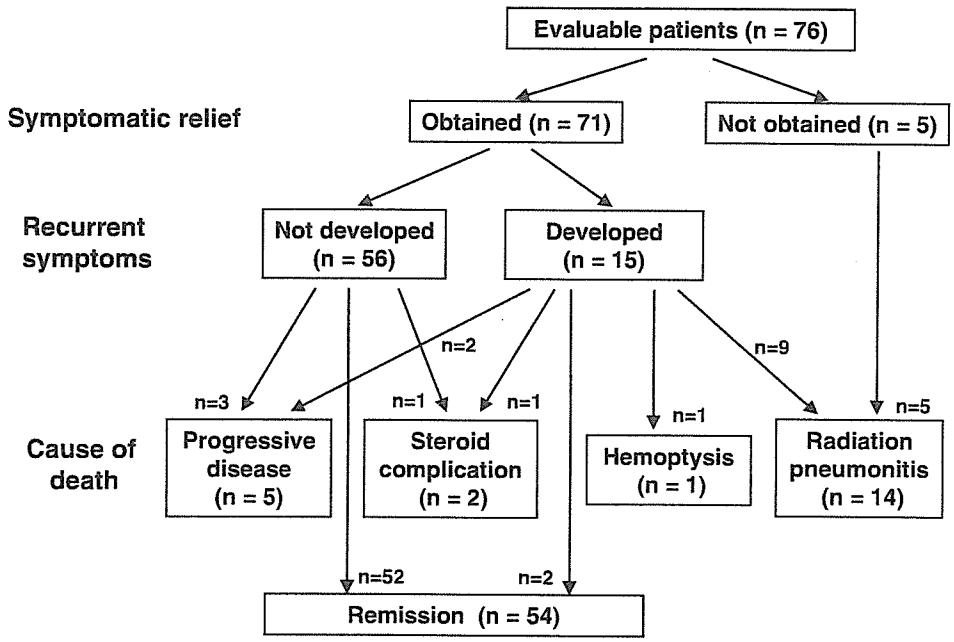

Fig. 1. Outcome of patients who received steroid therapy. Two patients were excluded because of loss of follow-up. Of 76 evaluable patients, 71 (93%) experienced symptomatic relief by steroid therapy.

tient and another in this study. This may be partly due to the diversity in clinical course of radiation pneumonitis, but mostly due to lacking in available recommendation for tapering schedules. In this study, median total duration of steroid therapy was 10 weeks, which may be a tentative guide. A guideline of taper schedule appeared in the latest textbook: the dose should be tapered by 10 mg every two weeks, and be terminated in 12 weeks [10].

Although our clinical practice mostly followed the expert opinions on the management of radiation-induced lung injury as mentioned above, there is little evidence that our steroid use, dose and duration for radiation-induced lung injury were correct. In this study, 21% of patients received steroid therapy and 4% of patients died of radiation pneumonitis among lung cancer patients treated with thoracic radiotherapy at a total dose of 50 Gy or higher. These figures are comparable to the incidence of grade 3 pneumonitis, 3–20%, and that of fatal pneumonitis, 1–4%, in other reports [10].

In conclusion, development of fever and dyspnea, and short interval between the end of radiotherapy and the first radiographic change were associated with fatal radiation-induced lung injury. Prednisolone 30–40 mg daily for two weeks followed by slow taper was selected for the treatment in many patients.

Acknowledgements

This work was supported in part by Grants-in-Aid for Cancer Research from the Ministry of Health, Labour and Welfare of Japan. We thank Yuko Yabe and Mika Nagai for preparation of the manuscript.

* **Corresponding author. Ikuo Sekine**, Division of Internal Medicine and Thoracic Oncology, National Cancer Center Hospital, Tsukiji 5-1-1, Chuo-ku, Tokyo 104-0045, Japan. *E-mail address:* isekine@ncc.go.jp

Received 11 October 2005; received in revised form 19 April 2006; accepted 23 May 2006; Available online 3 July 2006

References

[1] Groover TA, Christie AC, Merritt EA. Observations on the use of the copper filter in the roentgen treatment of deep-seated malignancies. South Med J 1922;15:440–4.
[2] Hines LE. Fibrosis of the lung following roentgen-ray treatments for tumor. JAMA 1922;79:720–2.
[3] Evans WA, Leucutia T. Intrathoracic changes induced by heavy radiation. Am J Roentgenol 1925;13:203–20.
[4] Gross NJ. Pulmonary effects of radiation therapy. Ann Intern Med 1977;86:81–92.
[5] Stover D, Kaner R. Pulmonary toxicity. In: DeVita Jr V, Hellman S, Rosenberg S, editors. Cancer: principles and practice of oncology. Philadelphia: Lippincott Williams & Wilkins; 2001. p. 2894–904.
[6] McDonald S, Rubin P, Phillips TL, Marks LB. Injury to the lung from cancer therapy: clinical syndromes, measurable endpoints, and potential scoring systems. Int J Radiat Oncol Biol Phys 1995;31:1187–203.
[7] Inoue A, Kunitoh H, Sekine I, et al. Radiation pneumonitis in lung cancer patients: a retrospective study of risk factors and the long-term prognosis. Int J Radiat Oncol Biol Phys 2001;49:649–55.
[8] Cosgriff SW, Kligerman MM. Use of ACTH and cortisone in the treatment of post-irradiation pulmonary reaction. Radiology 1951;57:536–40.
[9] Rubin P, Casarett GW. Clinical Radiation Pathology. Philadelphia: WB Saunders Co; 1968.
[10] Machtay M. Pulmonary complications of anticancer treatment. In: Abeloff M, Armitage JO, Niederhuber JE, Kastan MB, McKenna WG, editors. Clin. Oncol.. Philadelphia: Elsevier Churchill Livingstone; 2004. p. 1237–50.
[11] Pezner RD, Bertrand M, Cecchi GR, et al. Steroid-withdrawal radiation pneumonitis in cancer patients. Chest 1984;85:816–7.
[12] Parris TM, Knight JG, Hess CE, Constable WC. Severe radiation pneumonitis precipitated by withdrawal of corticosteroids: a diagnostic and therapeutic dilemma. Am J Roentgenol 1979;132:284–6.
[13] Castellino RA, Glatstein E, Turbow MM, et al. Latent radiation injury of lungs or heart activated by steroid withdrawal. Ann Intern Med 1974;80:593–9.